

# Halogenation at a Dimolybdenum(V) and Tungsten(V) Sulfur Bridge: Metallosulfenyl Halides $M_2(\mu\text{-SX})$ and $[M_2(\mu\text{-SX}_3)]_n$ . Charge-Transfer Interactions

June Q. Lee, Michael L. Sampson, John F. Richardson, and Mark E. Noble\*

Department of Chemistry, University of Louisville, Louisville, Kentucky 40292

Received June 23, 1995<sup>®</sup>

The reactions of halogens at anionic, radical, and neutral bridge sulfur sites within  $M_2S_2$  cores of various  $[M_2(\text{NAr})_2(\text{S}_2\text{P}(\text{OEt})_2)_2(\mu\text{-S})_2(\mu\text{-O}_2\text{CMe})]$  compounds ( $M = \text{Mo}, \text{W}$ ) produced covalent halosulfide ligands. Complexes containing the  $W_2(\mu\text{-SX})$  unit were obtained for  $X = \text{Cl}, \text{Br}, \text{and I}$ ; trihalide polymers of  $[M_2(\mu\text{-SX}_3)]_n$  units were obtained for  $M = \text{W}$  or  $\text{Mo}$  and  $X = \text{Br}$  or  $\text{I}$ . These latter compounds engaged in depolymerization equilibria in solution. The derivative containing the structural unit  $[Mo_2(\mu\text{-SI}_3)]_n$  undergoes photolysis in fluorescent light to  $I_2$  and a disulfide of the type  $Mo_2S\text{-}SMO_2$ . Crystallography of the  $W_2(\mu\text{-SBr})$  product clearly revealed the discrete bromosulfide bridge ligand,  $\mu\text{-SBr}$ . Crystallography of the  $[Mo_2(\mu\text{-SI}_3)]_n$  product revealed  $SX_3S^{3-}$  ligands which interconnected the  $Mo_2$  structural units into one-dimensional polymer chains. Simple charge transfer interactions between metallosulfur sites of various derivatives and iodine were also observed.

## Introduction

Halogenations of sulfur sites in organic and main group compounds have been known for a long time to produce isolable compounds which contain  $S\text{-}X$  bonds. Except for a few examples such as  $SF_6$ , compounds with  $S\text{-}X$  bonds are generally reactive, and some have considerable utility. Organic sulfenyl halides,  $RSX$ , are well-developed examples which can be synthesized by various means and which display a variety of reactions.<sup>1–12</sup> These sulfenyl halides find importance as organic synthetic reagents, as precursors to fungicides, and as representatives of biological sulfenyl halides in organisms as diverse as tobacco mosaic virus and humans.<sup>4–7,12,13</sup> Halogenated, main group, sulfur compounds are exemplified by simple sulfur-halogen binary species which include neutral and ionic derivatives,<sup>9–16</sup> although other main group examples are also known.<sup>17</sup>

In the organic sulfenyl halides and in many (but not all) main group compounds, the  $S\text{-}X$  bond is covalent and of nearly single bond order. The distinction is made between these  $S\text{-}X$  bonds and weaker interactions which can be extended to charge-transfer systems. The covalent vs charge transfer distinction is

not always clear, particularly in the cases of weak covalent and strong charge transfer situations.

Halogenations of sulfur sites within metallosulfur compounds could give metallosulfenyl halides,  $M_x(SX)$ , which contain halosulfide ligands. These reactions and product types are virtually unknown despite the considerable chemistry which has evolved in recent years for sulfur-based reactivity in metallosulfur systems. Several metallosulfur compounds have been particularly well characterized for such reactivity.<sup>18–27</sup> The metallosulfenyl halide complex  $M_x(SX)$  is distinct from the many metal–halide–sulfide compounds  $M_x(S)_y(X)_z$  which are known.<sup>28</sup>

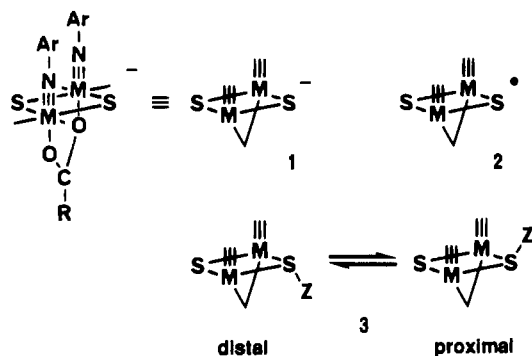
One of the sulfur-active metallosulfur systems which has been developed involves imidodithiophosphate–carboxylate derivatives of sulfidomolybdenum(V) compounds, typified by the anionic derivatives  $[Mo_2(\text{NAr})_2(\text{S}_2\text{P}(\text{OEt})_2)_2(\mu\text{-S})_2(\mu\text{-O}_2\text{CR})]^-$ , **1** ( $M = \text{Mo}$ ), and the radicals  $[Mo_2(\text{NAr})_2(\text{S}_2\text{P}(\text{OEt})_2)_2(\mu\text{-S})_2(\mu\text{-$

<sup>®</sup> Abstract published in *Advance ACS Abstracts*, September 15, 1995.

- (1) Kühle, E. *Synthesis* **1970**, 561.
- (2) Kühle, E. *Synthesis* **1971**, 563.
- (3) Kühle, E. *Synthesis* **1971**, 617.
- (4) Haas, A.; Niemann, U. *Adv. Inorg. Chem. Radiochem.* **1976**, *18*, 143.
- (5) Hogg, D. R. In *Comprehensive Organic Chemistry*; Jones, D. N., Ed.; Pergamon: Oxford, 1979; p 261.
- (6) Drabowicz, J.; Kielbasiński, P.; Mikołajczyk, M. In *The Chemistry of Sulphenic Acids and their Derivatives*; Patai, S., Ed.; Wiley & Sons: Chichester, England 1990; p 221.
- (7) Capozzi, G.; Modena, G.; Pasquato, L. In *The Chemistry of Sulphenic Acids and their Derivatives*; Patai, S., Ed.; Wiley & Sons: Chichester, England 1990; p 403.
- (8) Okuyama, T. In *The Chemistry of Sulphenic Acids and their Derivatives*; Patai, S., Ed.; Wiley & Sons: Chichester, England 1990; p 743.
- (9) Shreeve, J. M. In *Sulfur in Organic and Inorganic Chemistry*; Senning, A., Ed.; Marcel Dekker: New York, 1982; Vol. 4, p 131.
- (10) Hardstaff, W. R.; Langler, R. F. In *Sulfur in Organic and Inorganic Chemistry*; Senning, A., Ed.; Marcel Dekker: New York, 1982; Vol. 4, p 193.
- (11) Magee, P. S. In *Sulfur in Organic and Inorganic Chemistry*; Senning, A., Ed.; Marcel Dekker: New York, 1982; Vol. 4, p 283.
- (12) Field, L.; Lukehart, C. M. In *Sulfur in Organic and Inorganic Chemistry*; Senning, A., Ed.; Marcel Dekker: New York, 1982; Vol. 4, p 327.
- (13) Krebs, B.; Ahlers, F.-P. *Adv. Inorg. Chem.* **1990**, *35*, 235.

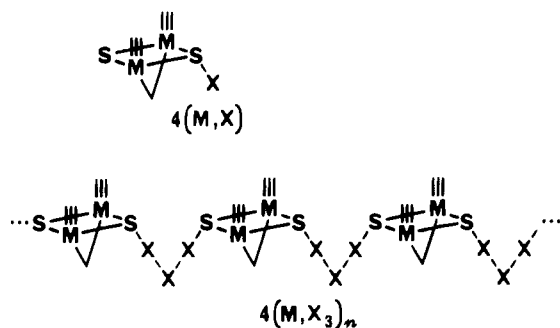
- (14) Klapötke, T.; Passmore, J. *Acc. Chem. Res.* **1989**, *22*, 234.
- (15) Murchie, M. P.; Johnson, J. P.; Passmore, J.; Sutherland, G. W.; Tajik, M.; Whidden, T. K.; White, P. S.; Grein, F. *Inorg. Chem.* **1992**, *31*, 273.
- (16) Bakshi, P.; Boyle, P. D.; Cameron, T. S.; Passmore, J.; Schatte, G.; Sutherland, G. W. *Inorg. Chem.* **1994**, *33*, 3849.
- (17) Burford, N.; Chivers, T.; Rao, M. N. S.; Richardson, J. F. *Inorg. Chem.* **1984**, *23*, 1946.
- (18) Rakowski-DuBois, M. *Chem. Rev.* **1989**, *89*, 1.
- (19) Birnbaum, J.; Godziela, G.; Maciejewski, M.; Tonker, T. L.; Haltiwanger, R. C.; Rakowski DuBois, M. *Organometallics* **1990**, *9*, 394.
- (20) Bernatis, P.; Haltiwanger, R. C.; Rakowski DuBois, M. *Organometallics* **1992**, *11*, 2435.
- (21) Lopez, L. L.; Gabay, J.; Haltiwanger, R. C.; Green, K.; Allshouse, J.; Casewit, C.; Rakowski DuBois, M. *Organometallics* **1993**, *12*, 4764.
- (22) Bolinger, C. M.; Rauchfuss, T. B. *Inorg. Chem.* **1982**, *21*, 3947.
- (23) Ruffing, C. J.; Rauchfuss, T. B. *Organometallics* **1985**, *4*, 524.
- (24) Giolando, D. M.; Rauchfuss, T. B.; Rheingold, A. L.; Wilson, S. R. *Organometallics* **1987**, *6*, 667.
- (25) Seyferth, D.; Henderson, R. S.; Song, L.-C.; Womack, G. B. *J. Organomet. Chem.* **1985**, *292*, 9.
- (26) Seyferth, D.; Womack, G. B.; Henderson, R. S.; Cowie, M.; Hames, B. W. *Organometallics* **1986**, *5*, 1568.
- (27) Cowie, M.; DeKock, R. L.; Wagenmaker, T. R.; Seyferth, D.; Henderson, R. S.; Gallagher, M. K. *Organometallics* **1989**, *8*, 119.
- (28) For examples for molybdenum and tungsten, see Fedorov, V. E.; Fedin, V. P.; Kuz'mina, O. A.; Semyannikov, P. P. *Russ. J. Inorg. Chem. (Engl. Transl.)* **1986**, *31*, 1456. Volkov, S. V.; Kolesnichenko, V. L.; Timoshchenko, N. I. *J. Coord. Chem.* **1988**, *17*, 367. Volkov, S. V.; Kolesnichenko, V. L.; Timoshchenko, N. I. *Russ. J. Inorg. Chem. (Engl. Transl.)* **1988**, *33*, 459.

$\text{O}_2\text{CR})^*$ , **2** ( $M = \text{Mo}$ ).<sup>29–33</sup> (Abbreviations of organic groups are given in ref 34. In the structure diagrams shown, dithiophosphate groups are omitted for clarity.) Anions **1** are potent



nucleophiles, while radicals **2** display sulfur-centered radical reactivity; these parallel thiolate  $\text{RS}^-$  and thiyl  $\text{RS}^\bullet$ , despite the very different bonding of dimolybdothiolate,  $\text{Mo}_2(\mu\text{-S})$ , and organosulfur,  $\text{RS}$ , sites. Recent investigations into sulfidotungsten(V) dimer anions  $[\text{W}_2(\text{NAr})_2(\text{S}_2\text{P}(\text{OEt})_2)_2(\mu\text{-S})_2(\mu\text{-O}_2\text{CR})]^-$ , **1** ( $M = \text{W}$ ), have shown some parallels to the molybdenum analog.<sup>35,36</sup> Common products of the various reactions are of the general formula  $[\text{M}_2(\text{NAr})_2(\text{S}_2\text{P}(\text{OEt})_2)_2(\mu\text{-S})(\mu\text{-O}_2\text{CR})(\mu\text{-SZ})]$ , **3**, and a considerable range of compounds has been characterized.

Given the importance of organic sulfenyl halides and the capability of sulfur-site reactivity in metallosulfur complexes, halogenations of the sulfur sites of anions **1** and radicals **2** were investigated in an effort to produce and characterize halosulfide complexes of the general type  $\text{M}_2(\mu\text{-SX})$ . Although organic  $\text{RSX}$  derivatives are well-known, halogenation of sulfur sites within these complexes was a more risky venture and constituted a more extreme test of durability for the  $\text{M}_2\text{S}_2$  core, considering that these dimers contain metals below their highest oxidation state and also contain co-ligands which are oxidizable. These reactions proved to be successful, however, and the characterization of metallosulfenyl halides, **4**( $M, X$ ), and trihalide polymers, **4**( $M, X_3$ )<sub>n</sub>, are described herein, along with charge transfer interactions also observed during the course of this study.



## Experimental Section

Reactions and manipulations were conducted open to air. *N*-Chlorosuccinimide was recrystallized from  $\text{CHCl}_3/\text{EtOH}$ /petroleum ether. Other commercial reagents were used as received. Syntheses of the

tetramers  $[\text{Mo}(\text{NTO})(\text{S}_2\text{P}(\text{OEt})_2)\text{S}]_4$  and  $[\text{W}(\text{NTO})(\text{S}_2\text{P}(\text{OEt})_2)\text{S}]_4$ ,<sup>35</sup> of the bis-dimer disulfide  $[\text{Mo}_2(\text{NTO})_2(\text{S}_2\text{P}(\text{OEt})_2)_2\text{S}_2(\text{O}_2\text{CMe})]_2$ , **5**,<sup>29</sup> and of the ethanethiolate-bridged dimer  $[\text{Mo}_2(\text{NTO})_2(\text{S}_2\text{P}(\text{OEt})_2)_2\text{S}(\text{O}_2\text{CMe})(\text{SEt})]$ , **3** ( $Z = \text{Et}$ ),<sup>30</sup> have been previously reported.  $^{31}\text{P}\{^1\text{H}\}$  and  $^1\text{H}$  NMR spectra were obtained on a Varian XL-300 spectrometer at 121 and 300 MHz and are reported as downfield shifts from external 85%  $\text{H}_3\text{PO}_4$  and internal  $\text{Me}_4\text{Si}$ . Infrared data were obtained by diffuse reflectance on KBr powder mixtures using a Mattson Galaxy Series FTIR 5000 spectrometer. UV-vis spectra were obtained as  $\text{CHCl}_3$  solutions using a Hewlett-Packard 8452A diode array spectrophotometer. All extinction coefficients are apparent values and do not necessarily correspond to peak positions unless noted; solution cell pathlengths were 1.0 or 0.10 cm.

Galbraith Laboratories, Inc. (Knoxville, TN) and Midwest Microlab (Indianapolis, IN) performed the elemental analyses. Results for Br and I analyses proved variable for compounds reported herein, even for repeat analyses of the same sample, even though C, H, and N results were excellent for the same sample. Despite the slight deviations from calculated values for Br and I, products were considered pure by the summation of data including spectroscopic characterization.

Preparative-scale photolysis was conducted in an apparatus consisting of four 20-W, 23-in., cool white fluorescent lamps. The lamps were arranged parallel and vertical, with the internal center of each lamp tube lying at the corners of a rectangle of dimensions 6.5 cm  $\times$  7.5 cm. The solution to photolyze was held parallel to the lamps, with the solution center near midlength of the lamps.

$[\text{W}_2(\text{NTO})_2(\text{S}_2\text{P}(\text{OEt})_2)_2\text{S}(\text{O}_2\text{CMe})(\text{SCl})]$ , **4**( $\text{W}, \text{Cl}$ ). *N*-Chlorosuccinimide (0.0242 g, 0.181 mmol) was added to a cold ( $-78^\circ\text{C}$  dry ice bath) solution of  $[\text{W}(\text{NTO})(\text{S}_2\text{P}(\text{OEt})_2)\text{S}]_4$  (0.1502 g, 0.0741 mmol),  $\text{MeCO}_2\text{H}$  (18  $\mu\text{L}$ , 0.33 mmol), and  $\text{Et}_3\text{N}$  (24  $\mu\text{L}$ , 0.18 mmol) in  $\text{CHCl}_3$  (1 mL). After being stirred for 5 min, the solution was removed from the dry ice bath and was stripped on a rotary evaporator. As the solution slowly warmed during the evaporation, the color abruptly changed from dark red to light yellow-orange. At room temperature, the residue was slurried in  $\text{MeOH}$ , filtered, and dried. The solid was redissolved in  $\text{CH}_2\text{Cl}_2$  (1 mL) and filtered.  $\text{EtOH}$  (4 mL) was added to the filtrate; the resulting slurry was filtered, and the solid was washed with  $\text{EtOH}/\text{H}_2\text{O}$  (2/1) and vacuum dried overnight to give an orange-red powder (0.1381 g, 84%). Anal. Calcd for  $\text{W}_2\text{C}_{24}\text{H}_{37}\text{N}_2\text{O}_6\text{P}_2\text{S}_6\text{Cl}$ : C, 26.0; H, 3.4; N, 2.5; S, 17.0; Cl, 3.2. Found: C, 25.8; H, 3.1; N, 2.4; S, 17.0; Cl, 3.0.  $^{31}\text{P}$  NMR (ppm): 123.8;  $^2J_{\text{PW}} = 22$  Hz,  $^3J_{\text{PW}} = 9$  Hz.  $^1\text{H}$  NMR (ppm): 6.50 d, 6.41 d,  $\text{To-H}$ ; 4.3–4.0 m,  $\text{POCH}_2$ ; 2.11 s,  $\text{To-CH}_3$ ; 1.36 t, 1.22 t,  $\text{POCCH}_3$ ; 1.35 s,  $\text{O}_2\text{CCH}_3$ . IR ( $\text{cm}^{-1}$ ): 1537 m, 1458 s, 1007 vs, 968 s, 819 s, 797 m, 473 w.

$[\text{W}_2(\text{NTO})_2(\text{S}_2\text{P}(\text{OEt})_2)_2\text{S}(\text{O}_2\text{CMe})(\text{SBr})]$ , **4**( $\text{W}, \text{Br}$ ).  $\text{Br}_2$  (16  $\mu\text{L}$ , 0.31 mmol) was added to a chilled (ice/salt bath) solution of  $[\text{W}(\text{NTO})(\text{S}_2\text{P}(\text{OEt})_2)\text{S}]_4$  (0.1503 g, 0.0741 mmol),  $\text{MeCO}_2\text{H}$  (18  $\mu\text{L}$ , 0.33 mmol), and  $\text{Et}_3\text{N}$  (24  $\mu\text{L}$ , 0.18 mmol) in  $\text{CHCl}_3$  (2 mL). The solution was stirred while cold for 5 min and then stripped to dryness on a rotary evaporator. A modest color change from dark red to a lighter red occurred during evaporation as the solution slowly warmed. The residue was slurried in  $\text{MeOH}$  at room temperature, filtered, and dried. The solid was redissolved in  $\text{CH}_2\text{Cl}_2$  (1 mL) and filtered.  $\text{EtOH}$  (4 mL) was added to the filtrate to precipitate the product which was collected (filtration), washed with  $\text{EtOH}/\text{H}_2\text{O}$  (2/1) and vacuum dried overnight to give an orange-red powder (0.1264 g, 72%).  $^{31}\text{P}$  NMR (ppm): 122.4;  $^2J_{\text{PW}} = 22$  Hz,  $^3J_{\text{PW}} = 8$  Hz.  $^1\text{H}$  NMR (ppm): 6.51 d, 6.42 d,  $\text{To-H}$ ; 4.3–4.0 m,  $\text{POCH}_2$ ; 2.11 s,  $\text{To-CH}_3$ ; 1.36 s,  $\text{O}_2\text{CCH}_3$ ; 1.36 t, 1.22 t,  $\text{POCCH}_3$ . IR ( $\text{cm}^{-1}$ ): 1535 m, 1458 s, 1007 vs, 968 s, 819 s, 770 m.

An alternate reaction was as follows. *N*-Bromophthalimide (0.0402 g, 0.178 mmol) was added to a cold (ice/salt bath) solution of  $[\text{W}(\text{NTO})(\text{S}_2\text{P}(\text{OEt})_2)\text{S}]_4$  (0.1501 g, 0.0741 mmol),  $\text{MeCO}_2\text{H}$  (18  $\mu\text{L}$ , 0.33 mmol), and  $\text{Et}_3\text{N}$  (24  $\mu\text{L}$ , 0.18 mmol) in  $\text{CHCl}_3$  (1 mL). After cold stirring for 5 min, the solution was removed from the ice bath and then stripped (starting cold) to dryness on a rotary evaporator. The residue was slurried in  $\text{MeOH}$  at room temperature, filtered and dried. The solid was redissolved in  $\text{CH}_2\text{Cl}_2$  (1 mL) and filtered.  $\text{EtOH}$  (4 mL) was added to the filtrate; the resulting slurry was filtered, and the precipitate was washed with  $\text{EtOH}/\text{H}_2\text{O}$  (2/1) and vacuum dried. Two additional recrystallizations from  $\text{CH}_2\text{Cl}_2/\text{EtOH}/\text{H}_2\text{O}$  yielded product (0.1195 g, 71%) which still contained some impurities ( $\sim 4\%$ ).

(29) Noble, M. E. *Inorg. Chem.* **1986**, *25*, 3311.

(30) Noble, M. E. *Inorg. Chem.* **1987**, *26*, 877.

(31) Lizano, A. C.; Noble, M. E. *Inorg. Chem.* **1988**, *27*, 747.

(32) Lizano, A. C.; Munchhof, M. G.; Haub, E. K.; Noble, M. E. *J. Am. Chem. Soc.* **1991**, *113*, 9204.

(33) Haub, E. K.; Lizano, A. C.; Noble, M. E. *J. Am. Chem. Soc.* **1992**, *114*, 2218.

(34) Abbreviations used in this paper: Me, methyl; Et, ethyl; Ar, aryl; Ph, phenyl; To, *p*-tolyl; NXS, *N*-halosuccinimide; NHS, succinimide.

(35) Sampson, M. L.; Richardson, J. F.; Noble, M. E. *Inorg. Chem.* **1992**, *31*, 2726.

(36) Sampson, M. L.; Richardson, J. F.; Noble, M. E. Work in progress.

$[\text{W}_2(\text{NTO})_2(\text{S}_2\text{P}(\text{OEt})_2)_2\text{S}(\text{O}_2\text{CMe})(\text{SI})]_n$ , **4(W,I)**. A solution of  $[\text{W}(\text{NTO})(\text{S}_2\text{P}(\text{OEt})_2)\text{S}]_4$  (0.1503 g, 0.0741 mmol),  $\text{MeCO}_2\text{H}$  (18  $\mu\text{L}$ , 0.33 mmol), and  $\text{Et}_3\text{N}$  (24  $\mu\text{L}$ , 0.18 mmol) in  $\text{CHCl}_3$  (2 mL) was treated with  $\text{I}_2$  (0.0764 g, 0.30 mmol) and then stirred for 5 min. After rotary evaporation of the solution to dryness, the residue was slurried in  $\text{MeOH}$ , filtered, and dried. The solid was redissolved in  $\text{CH}_2\text{Cl}_2$  (1 mL) and the solution was filtered. Petroleum ether (6 mL) was added to the filtrate; the resulting precipitate was collected, washed with petroleum ether and vacuum dried overnight. The product was an orange powder (0.1651 g, 92%). Anal. Calcd for  $\text{W}_2\text{C}_{24}\text{H}_{37}\text{N}_2\text{O}_6\text{P}_2\text{S}_6\text{I}$ : C, 24.1; H, 3.1; N, 2.3; I, 10.6. Found: C, 24.1; H, 3.0; N, 2.0; I, 11.6.  $^{31}\text{P}$  NMR (ppm): 119.7;  $^2J_{\text{PW}} = 21$  Hz,  $^3J_{\text{PW}} \sim 8$  Hz.  $^1\text{H}$  NMR (ppm): 6.50 d, 6.42 d, To-H; 4.3–4.0 m,  $\text{POCH}_2$ ; 2.10 s, To- $\text{CH}_3$ ; 1.40 s,  $\text{O}_2\text{CCH}_3$ ; 1.37 t, 1.22 t,  $\text{POCCH}_3$ . IR ( $\text{cm}^{-1}$ ): 1539 m, 1454 s, 1009 vs, 964 s, 818 s, 793 m.

$[\text{W}_2(\text{NTO})_2(\text{S}_2\text{P}(\text{OEt})_2)_2\text{S}(\text{O}_2\text{CMe})(\text{SI}_3)]_n$ , **4(W,I\_3)**. A solution of  $[\text{W}(\text{NTO})(\text{S}_2\text{P}(\text{OEt})_2)\text{S}]_4$  (0.1502 g, 0.0741 mmol),  $\text{MeCO}_2\text{H}$  (18  $\mu\text{L}$ , 0.33 mmol), and  $\text{Et}_3\text{N}$  (24  $\mu\text{L}$ , 0.18 mmol) in  $\text{CH}_2\text{Cl}_2$  (2 mL) was treated with  $\text{I}_2$  (0.764 g, 3.0 mmol). Product precipitated as the solution was stirred for 10 min. The slurry was filtered, and the solid was washed ( $\text{MeOH}$ ). This was redissolved in  $\text{CH}_2\text{Cl}_2$  (1 mL) and filtered. Petroleum ether (8 mL) was added to the filtrate and the resulting precipitate was collected (filtration), washed (petroleum ether), and vacuum dried overnight to give an orange powder (0.1893 g, 88%). Anal. Calcd for  $\text{W}_2\text{C}_{24}\text{H}_{37}\text{N}_2\text{O}_6\text{P}_2\text{S}_6\text{I}_3$ : C, 19.8; H, 2.6; N, 1.9; I, 26.2. Found: C, 19.5; H, 2.6; N, 2.0; I, 24.7.  $^{31}\text{P}$  NMR (ppm): 117.8;  $^2J_{\text{PW}} = 22$  Hz,  $^3J_{\text{PW}} \sim 6$  Hz.  $^1\text{H}$  NMR (ppm): 6.52 s, To-H (all degenerate); 4.3–4.0 m,  $\text{POCH}_2$ ; 2.12 s, To- $\text{CH}_3$ ; 1.44 s,  $\text{O}_2\text{CCH}_3$ ; 1.40 t, 1.22 t,  $\text{POCCH}_3$ . IR ( $\text{cm}^{-1}$ ): 1534 m, 1454 s, 1011 vs, 970 s, 818 s, 797 m.

$[\text{Mo}_2(\text{NTO})_2(\text{S}_2\text{P}(\text{OEt})_2)_2\text{S}(\text{O}_2\text{CMe})(\text{SBr}_3)]_n$ , **4(Mo,Br\_3)**. A solution of the bis-dimer disulfide  $[\text{Mo}_2(\text{NTO})_2(\text{S}_2\text{P}(\text{OEt})_2)_2\text{S}_2(\text{O}_2\text{CMe})]_2$ , **5**, (0.0590 g, 0.033 mmol) and 1.0%  $\text{Br}_2/\text{CHCl}_3$  (0.68 mL, 0.13 mmol) in  $\text{CHCl}_3$  (2 mL) was stirred for 10 min. The solution was then stripped on a rotary evaporator to remove excess  $\text{Br}_2$ . The orange residue was dissolved in  $\text{CH}_2\text{Cl}_2$  (0.5 mL). Petroleum ether (10 mL) was added slowly to precipitate product. The slurry was filtered; the product was washed (petroleum ether) and vacuum dried to give an orange powder (0.0596 g, 80%). Anal. Calcd for  $\text{Mo}_2\text{C}_{24}\text{H}_{37}\text{N}_2\text{O}_6\text{P}_2\text{S}_6\text{Br}_3$ : C, 25.4; H, 3.3; N, 2.5; Br, 21.1. Found: C, 25.1; H, 3.1; N, 2.5; Br, 20.1.  $^{31}\text{P}$  NMR (ppm): 110.2.  $^1\text{H}$  NMR (ppm): 6.99 d, 6.62 d, To-H; 4.18 dq, 4.02 dq,  $\text{POCH}_2$ ; 2.14 s, To- $\text{CH}_3$ ; 1.39 s,  $\text{O}_2\text{CCH}_3$ ; 1.37 t, 1.20 t,  $\text{POCCH}_3$ . IR ( $\text{cm}^{-1}$ ): 1520 m, 1451 s, 1008 vs, 970 s, 816 s, 799 s.

$[\text{Mo}_2(\text{NTO})_2(\text{S}_2\text{P}(\text{OEt})_2)_2\text{S}(\text{O}_2\text{CMe})(\text{SI}_3)]_n$ , **4(Mo,I\_3)**. A solution of the bis-dimer disulfide  $[\text{Mo}_2(\text{NTO})_2(\text{S}_2\text{P}(\text{OEt})_2)_2\text{S}_2(\text{O}_2\text{CMe})]_2$ , **5**, (0.1081 g, 0.0603 mmol) and  $\text{I}_2$  (0.0614 g, 0.24 mmol) in  $\text{CHCl}_3$  (2.0 mL) was photolyzed in an NMR tube for 20 h. The resulting slurry was filtered; the solid product was rinsed lightly with  $\text{CHCl}_3$ , and vacuum dried overnight to give an orange powder (0.1108 g, 72%).  $^{31}\text{P}$  NMR (ppm): 109.3.  $^1\text{H}$  NMR (ppm): 6.85 d, 6.57 d, To-H; 4.19 dq, 4.04 dq,  $\text{POCH}_2$ ; 2.13 s, To- $\text{CH}_3$ ; 1.40 s,  $\text{O}_2\text{CCH}_3$ ; 1.37 t, 1.21 t,  $\text{POCCH}_3$ . IR ( $\text{cm}^{-1}$ ): 1532 m, 1449 s, 1009 vs, 966 s, 816 s, 793 m.

$[\text{W}_2(\text{NTO})_2(\text{S}_2\text{P}(\text{OEt})_2)_2\text{S}(\text{O}_2\text{CMe})(\text{SEt})]_n$ , **3 (Z = Et)**. The synthesis parallels those of related derivatives.<sup>29,30</sup> To a solution of  $[\text{W}(\text{NTO})(\text{S}_2\text{P}(\text{OEt})_2)\text{S}]_4$  (0.1506 g, 0.0741 mmol),  $\text{MeCO}_2\text{H}$  (18  $\mu\text{L}$ , 0.33 mmol), and  $\text{Et}_3\text{N}$  (24  $\mu\text{L}$ , 0.18 mmol) in  $\text{CHCl}_3$  (2 mL) was added  $\text{EtBr}$  (11  $\mu\text{L}$ , 1.5 mmol). After 20 min of stirring, the solution was stripped to dryness on a rotary evaporator. The resulting residue was dissolved in  $\text{THF}$  and filtered; the filtrate was treated with 2/1  $\text{MeOH}/\text{H}_2\text{O}$ . The slurry was filtered, and the precipitate was washed with 4/1  $\text{MeOH}/\text{H}_2\text{O}$  and then vacuum-dried overnight to give a yellow crystalline product (0.097 g, 59%). Anal. Calcd for  $\text{W}_2\text{C}_{26}\text{H}_{42}\text{N}_2\text{O}_6\text{P}_2\text{S}_6$ : C, 28.4; H, 3.8; N, 2.5. Found: C, 27.8; H, 4.1; N, 2.4.  $^{31}\text{P}$  NMR (ppm): 127.5,  $^2J_{\text{PW}} = 23$  Hz,  $^3J_{\text{PW}} = 11$  Hz; 127.2 (minor invertomer),  $^2J_{\text{PW}} = 23$  Hz,  $^3J_{\text{PW}} = 10$  Hz.  $^1\text{H}$  NMR (ppm): minor invertomer peaks are in parentheses where discernible): 6.57 d, 6.47 d, (6.36 d), To-H; 4.3–4.0 m,  $\text{POCH}_2$ ; 3.24 q, (2.25 q),  $\text{SCH}_2$ ; 2.13 s, (2.08 s), To- $\text{CH}_3$ ; 1.83 t,  $\text{SCCH}_3$ ; 1.4–1.1 m,  $\text{POCCH}_3 + \text{O}_2\text{CCH}_3$ . IR ( $\text{cm}^{-1}$ ): 1532 m, 1445 s, 1007 vs, 965 s, 822 s, 783 m.

**Derivations Using UV-Vis Spectral Data.** Support for the equilibrium described in the Results was derived from UV-vis spectral

data as follows. For the three equilibrium species of eq 12 (in Results), the total absorbance at a specific wavelength is given by eq 1, where

$$A = \{\epsilon_A c_A + \epsilon_B c_B + \epsilon_C c_C\} b \quad (1)$$

$$A = \{\epsilon_B + \epsilon_C\} c_B b \quad (2)$$

$$\frac{A_{410}}{A_{510}} = \frac{\{\epsilon_{B,410} + \epsilon_{C,410}\}}{\{\epsilon_{B,510} + \epsilon_{C,510}\}} \quad (3)$$

compounds  $A = [\text{Mo}_2\text{SI}_3]_n$ ,  $B = \text{Mo}_2\text{SI}$ , and  $C = \text{I}_2$ . In the case of  $[\text{Mo}_2\text{SI}_3]_n$ , the parameters are per  $\text{Mo}_2$  unit:  $c_A$  is the total concentration of  $\text{Mo}_2$  units in polymer chains, and  $\epsilon_A$  is the extinction coefficient per  $\text{Mo}_2$  unit in the polymer chain. (An assumption in these methods is that all polymers and oligomers have the same spectral features per  $\text{Mo}_2$  unit.) At sufficiently high dilution, depolymerization is favored, the concentration of  $[\text{Mo}_2\text{SI}_3]_n$  becomes negligible and  $\epsilon_{ACA} \ll \epsilon_{BCB}$ ; the absorbance (eq 1) is then due to  $\text{Mo}_2\text{SI}$  and  $\text{I}_2$  only. (This was valid since  $\epsilon_A$  was within the same order of magnitude as  $\epsilon_B$  at the selected wavelengths.) Also, for the experimental conditions for eq 12,  $c_B = c_C$ . These considerations lead to eq 2. An absorbance ratio at 410 and 510 nm is defined and calculated as per eq 3 for different solution concentrations.

For the equilibrium of eq 13 (in Results), only two species,  $[\text{Mo}_2\text{SI}_3]_n$  and  $\text{Mo}_2\text{SI}_3$ , are in solution and the total absorbance is given by eq 4, where  $A = [\text{Mo}_2\text{SI}_3]_n$  and  $D = \text{Mo}_2\text{SI}_3$ . At high dilution,  $\epsilon_{ACA} \ll \epsilon_{DCD}$ ; absorbance is due to  $\text{Mo}_2\text{SI}_3$  only, and the absorbance ratio at 410 and 510 nm reduces to eq 5.

$$A = \{\epsilon_A c_A + \epsilon_D c_D\} b \quad (4)$$

$$\frac{A_{410}}{A_{510}} = \frac{\epsilon_{D,410}}{\epsilon_{D,510}} \quad (5)$$

UV-vis spectral parameters of nine  $[\text{Mo}_2(\text{NTO})_2(\text{S}_2\text{P}(\text{OEt})_2)_2\text{S}(\text{O}_2\text{CMe})(\text{SZ})]_n$  derivatives, **3**, have been previously reported;<sup>32</sup> the spectral parameters of these compounds were similar regardless of the functionality of Z (Z = R, SR, or  $\text{NH}_2$ ). Since the values were similar regardless of Z and since  $\text{Mo}_2\text{SI}$  and  $\text{Mo}_2\text{SI}_3$  are structurally equivalent to such compounds **3**, values of  $\epsilon_{410}$  ( $5900\text{--}7450 \text{ cm}^{-1} \text{ M}^{-1}$ ) and  $\epsilon_{510}$  ( $1340\text{--}1500 \text{ cm}^{-1} \text{ M}^{-1}$ ) from those prior derivatives were considered representative of the corresponding  $\epsilon$  values for  $\text{Mo}_2\text{SI}$  (B) in eq 3 and for  $\text{Mo}_2\text{SI}_3$  (D) in eq 5. The  $\epsilon$  values for  $\text{I}_2$  ( $\epsilon_C$  in eqs 1–3) were separately measured to be  $42 \text{ cm}^{-1} \text{ M}^{-1}$  at 410 nm and  $938 \text{ cm}^{-1} \text{ M}^{-1}$  at 510 nm. Values for  $A_{410}/A_{510}$  in eqs 3 and 5 were then calculated using the  $\text{I}_2$  data and the values for the prior compounds **3**: these ratios averaged 2.8 ( $\sigma = 0.3$ ; range, 2.4–3.2) for eq 3 and 4.7 ( $\sigma = 0.4$ ; range, 3.9–5.3) for eq 5. These values were cleanly separated since the contribution from  $\text{I}_2$  was trivial to the numerator but substantial to the denominator of eq 3, thereby decreasing the ratio significantly.

The observed values of  $A_{410}/A_{510}$  for actual solutions of  $[\text{Mo}_2\text{SI}_3]_n$ , progressed smoothly from 3.7 at  $1.00 \times 10^{-3} \text{ F}$  to 3.2 at  $1.00 \times 10^{-5} \text{ F}$  (which was the lowest concentration which could be reliably measured). Dilution clearly tended toward the value for eq 3 involving free  $\text{I}_2$ .

**Photolysis Study.** The photolysis of  $[\text{Mo}_2(\text{NTO})_2(\text{S}_2\text{P}(\text{OEt})_2)_2\text{S}(\text{O}_2\text{CMe})(\text{SI}_3)]_n$ , **4(Mo,I\_3)**, was studied using 7.07 mg of the compound in 1.0 mL of  $\text{CDCl}_3$  in an NMR tube. This was photolyzed in a light box using a 22-W, 8-in., circular fluorescent lamp as previously described.<sup>32</sup> NMR spectra were obtained at various photolysis time intervals. The reverse photolysis from the bis-dimer disulfide  $[\text{Mo}_2(\text{NTO})_2(\text{S}_2\text{P}(\text{OEt})_2)_2\text{S}_2(\text{O}_2\text{CMe})]_2$ , **5**, and  $\text{I}_2$  was conducted using equivalent quantities as for  $[\text{Mo}_2(\text{NTO})_2(\text{S}_2\text{P}(\text{OEt})_2)_2\text{S}(\text{O}_2\text{CMe})(\text{SI}_3)]_n$  and the same light source.

**Charge Transfer Studies.** The primary studies were conducted using  $[\text{Mo}_2(\text{NTO})_2(\text{S}_2\text{P}(\text{OEt})_2)_2\text{S}(\text{O}_2\text{CMe})(\text{SEt})]_n$ , **3 (Z = Et)** and varying  $\text{I}_2$  ratios. For each sample,  $[\text{Mo}_2(\text{NTO})_2(\text{S}_2\text{P}(\text{OEt})_2)_2\text{S}(\text{O}_2\text{CMe})(\text{SEt})]_n$  (0.0324 mmol), 0.0394 M  $\text{I}_2$  in  $\text{CDCl}_3$ , and additional  $\text{CDCl}_3$  were

**Table 1.** Crystallographic Data

	4(W,Br)	4(Mo,I <sub>3</sub> ) <sub>n</sub>
formula	W <sub>2</sub> C <sub>24</sub> H <sub>37</sub> BrN <sub>2</sub> O <sub>6</sub> P <sub>2</sub> S <sub>6</sub>	Mo <sub>2</sub> C <sub>24</sub> H <sub>37</sub> N <sub>2</sub> O <sub>6</sub> P <sub>2</sub> S <sub>6</sub> I <sub>3</sub>
fw	1151.5	1276.50
space group	P1̄ (No. 2)	P2 <sub>1</sub> /c (No. 14)
a, Å	14.031(3)	10.870(3)
b, Å	14.564(3)	21.308(5)
c, Å	11.091(3)	18.900(5)
α, deg	105.75(2)	
β, deg	108.75(2)	99.11(2)
γ, deg	105.14(2)	
T, °C	23(1)	23(1)
V, Å <sup>3</sup>	1909.8	4322.2
Z	2	4
λ, Å	0.710 73 (Mo Kα)	0.710 73 (Mo Kα)
ρ <sub>calc</sub> , g cm <sup>-3</sup>	2.00	1.96
μ, cm <sup>-1</sup>	76.2	30.7
transm coeff (min/max)	0.568/0.999	0.923/1.000
octants	±h, -k, ±l	-h, -k, ±l
no. of reflns measd	7026	8261
no. of reflns with I > 3σ(I)	6727	5281
Δ(ρ), e Å <sup>-3</sup>	0.57	0.87
R <sup>a</sup>	0.034	0.038
R <sub>w</sub> <sup>b</sup>	0.037	0.041
agreement est	0.055	0.021

$$^a R = \sum ||F_o| - |F_c|| / \sum |F_o|, \quad ^b R_w = [\sum w(|F_o| - |F_c|)^2 / \sum w|F_o|^2]^{1/2}.$$

combined so as to provide the desired quantity of I<sub>2</sub> and a total solution volume of 1.0 mL.

**Crystallography.** The crystal data and experimental details are given in Table 1. Data were collected on an Enraf-Nonius CAD4 automated diffractometer with Mo Kα radiation (graphite monochromator), using the ω-2θ scan technique; computations utilized the Enraf-Nonius VAX/MoLEN programs.<sup>37</sup> Three representative reflections were measured every 60 min; their intensities remained constant within experimental error. Lorentz and polarization corrections were applied to the data. Scattering and anomalous dispersion factors were taken from ref 38.

For 4(W,Br), a red-orange, cut, block crystal from CHCl<sub>3</sub>/i-PrOH measuring 0.40 × 0.40 × 0.46 mm was used for data collection. Cell constants and an orientation matrix were obtained from least-squares refinement of 25 reflections. An empirical absorption correction (ψ data) was applied.

The structure was solved using the Patterson method, which revealed the positions of the two tungsten atoms. The remaining atoms were located in succeeding difference Fourier syntheses. One ethoxy group and one ethyl group of separate dithiophosphates were disordered: O(3)-C(17)-C(18) was modeled as two O-C-C groups in the ratio of 0.6:0.4; C(23)-C(24) was modeled as two C-C groups in the ratio of 0.6:0.4. Hydrogen atoms were located and added to the structure factor calculations but their parameters were not refined. The structure was refined in full-matrix least-squares, minimizing  $\sum w(|F_o| - |F_c|)^2$  where  $w = [\sigma^2(F) + (0.010F)^2 + 0.6]^{-1}$ . Selected results are given in Tables 2 and 3, and the structure is shown in Figure 1.

Crystals of 4(Mo,I<sub>3</sub>)<sub>n</sub> were obtained by layering n-C<sub>12</sub>H<sub>26</sub> (2 mL) onto a solution of 4(Mo,I<sub>3</sub>)<sub>n</sub> (6.1 mg) and I<sub>2</sub> (5.3 mg) in C<sub>6</sub>H<sub>5</sub>Cl (1 mL) and allowing 3 days for diffusion while it was kept in a black box. A red plate crystal measuring 0.08 × 0.18 × 0.22 mm was used for data collection. Cell constants and an orientation matrix were obtained from least-squares refinement of 25 reflections. An empirical absorption correction (ψ data) was applied.

The structure was solved by direct methods which revealed the positions of the two molybdenum and the three iodine atoms. The remaining atoms were located in succeeding difference Fourier syntheses. Several dithiophosphate ethyl groups were disordered: two

**Table 2.** Selected Bond Lengths (Å)

	4(W,Br)	4(Mo,I <sub>3</sub> ) <sub>n</sub>
M(1)-M(2)	2.8315(6)	2.878(1)
M(1)-S(1)	2.417(3)	2.442(2)
M(1)-S(2)	2.351(3)	2.413(2)
M(1)-S(3)	2.504(3)	2.501(3)
M(1)-S(4)	2.536(3)	2.517(3)
M(1)-O(1)	2.187(4)	2.159(5)
M(1)-N(1)	1.743(5)	1.733(6)
M(2)-S(1)	2.427(3)	2.438(2)
M(2)-S(2)	2.350(3)	2.413(2)
M(2)-S(5)	2.495(3)	2.504(3)
M(2)-S(6)	2.542(3)	2.515(3)
M(2)-O(2)	2.177(4)	2.160(5)
M(2)-N(2)	1.753(5)	1.748(6)
S(3)-P(1)	1.999(5)	2.004(4)
S(4)-P(1)	1.977(5)	2.006(4)
S(5)-P(2)	1.991(5)	1.997(4)
S(6)-P(2)	1.997(5)	1.995(4)
O(1)-C(15)	1.24(1)	1.280(9)
O(2)-C(15)	1.246(9)	1.25(1)
N(1)-C(1)	1.390(8)	1.374(9)
N(2)-C(8)	1.383(7)	1.370(9)
Br-S(1)	2.209(2)	
I(1)-I(2)		3.1584(7)
I(1)-S(1)		2.498(2)
I(2)-I(3)		3.0363(8)
I(3)-S(2)		2.544(2)

**Table 3.** Selected Bond Angles (deg)

	4(W,Br)	4(Mo,I <sub>3</sub> ) <sub>n</sub>
S(1)-M(1)-S(2)	107.32(9)	107.09(8)
S(1)-M(1)-S(4)	87.9(1)	88.18(8)
S(2)-M(1)-S(3)	84.8(1)	84.14(8)
S(3)-M(1)-S(4)	78.0(1)	79.09(8)
O(1)-M(1)-N(1)	173.0(3)	176.1(2)
M(2)-M(1)-O(1)	81.2(2)	80.7(1)
M(2)-M(1)-N(1)	99.3(2)	96.8(2)
S(1)-M(2)-S(2)	107.02(9)	107.20(8)
S(1)-M(2)-S(6)	89.65(9)	87.90(8)
S(2)-M(2)-S(5)	83.1(1)	84.20(7)
S(5)-M(2)-S(6)	78.5(1)	79.28(8)
O(2)-M(2)-N(2)	171.4(3)	178.0(2)
M(1)-M(2)-O(2)	82.3(2)	81.9(1)
M(1)-M(2)-N(2)	98.0(3)	98.1(2)
M(1)-S(1)-M(2)	71.54(7)	72.30(6)
M(1)-S(2)-M(2)	74.08(8)	73.23(6)
M(1)-S(3)-P(1)	88.1(2)	87.8(1)
M(1)-S(4)-P(1)	87.7(2)	87.3(1)
M(2)-S(5)-P(2)	87.9(1)	87.0(1)
M(2)-S(6)-P(2)	86.5(1)	86.8(1)
S(3)-P(1)-S(4)	105.9(2)	105.7(2)
S(5)-P(2)-S(6)	106.1(2)	106.6(2)
M(1)-O(1)-C(15)	126.5(4)	127.4(5)
M(2)-O(2)-C(15)	125.5(5)	126.6(5)
M(1)-N(1)-C(1)	178.4(7)	174.0(6)
M(2)-N(2)-C(8)	176.6(7)	176.5(5)
O(1)-C(15)-O(2)	124.7(5)	123.4(6)
W(1)-S(1)-Br	112.83(8)	
W(2)-S(1)-Br	114.68(9)	
Mo(1)-S(1)-I(1)		115.38(9)
Mo(2)S(1)-I(1)		115.84(9)
Mo(1)-S(2)-I(3)		114.89(8)
Mo(2)-S(2)-I(3)		115.02(8)
S(1)-I(1)-I(2)		171.65(5)
S(2)-I(3)-I(2)		172.56(4)
I(1)-I(2)-I(3)		83.89(2)

C(17) sites (0.8:0.2), three C(18) sites (0.6:0.2:0.2), two C(19) sites (0.6:0.4), two C(20) sites (0.6:0.4), and two C(24) sites (0.6:0.4) were modeled in the ratios shown parenthetically. Hydrogen atoms were located and added to the structure factor calculations but their parameters were not refined. The structure was refined in full-matrix least-squares, minimizing  $\sum w(|F_o| - |F_c|)^2$  where  $w = [\sigma^2(F) + (0.010F)^2 + 0.1]^{-1}$ . Selected results are in Tables 2 and 3, and the structure is shown in Figures 2 and 3.

(37) *MolEN, An Interactive Structure Solution Procedure*; Enraf-Nonius: Delft, The Netherlands, 1990.

(38) *International Tables for X-Ray Crystallography*; Kynoch: Birmingham, England, 1974; Vol. IV, Tables 2.2B, 2.3.1.

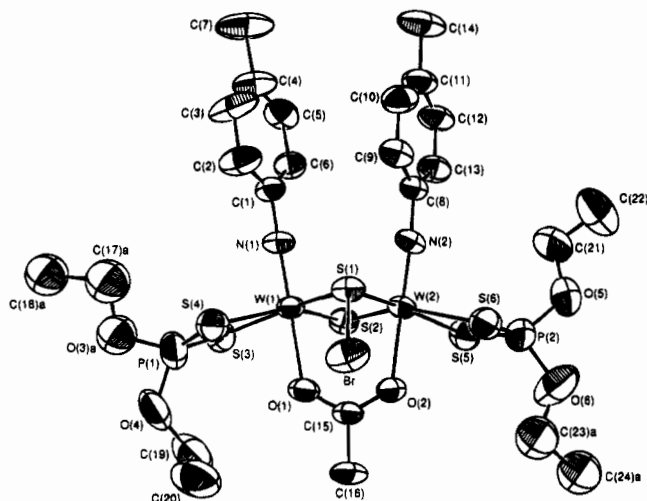


Figure 1. ORTEP view of  $[W_2(NTO)_2(S_2P(OEt)_2)_2S(O_2CMe)(SBr)]_4(W,Br)$ .

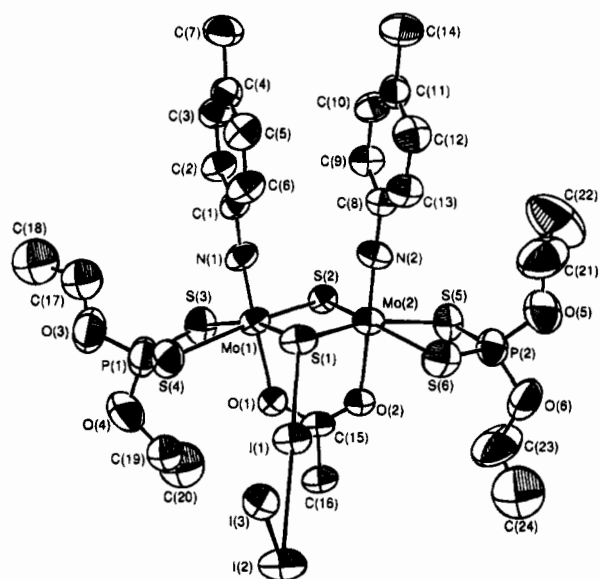


Figure 2. ORTEP view of one repeat unit of  $[Mo_2(NTO)_2(S_2P(OEt)_2)_2S(O_2CMe)(SI_3)]_n$ .

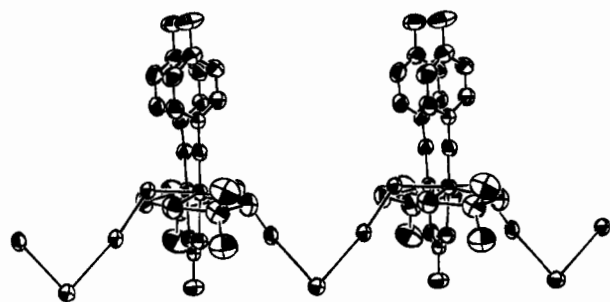


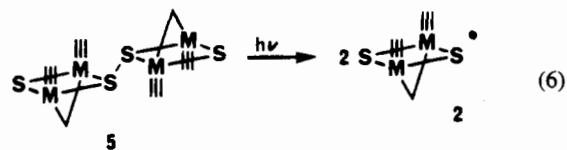
Figure 3. ORTEP view of the polymer chain of  $[Mo_2(NTO)_2(S_2P(OEt)_2)_2S(O_2CMe)(SI_3)]_n$ . The ethyl groups of dithiophosphate ligands are omitted for clarity.

## Results

For simplicity,  $[M_2(NTO)_2(S_2P(OEt)_2)_2S_2(O_2CMe)]$  dimer groups are designated  $M_2S^-$ , wherein the S represents one sulfur bridge. Abbreviations for organic groups have been footnoted.<sup>34</sup>

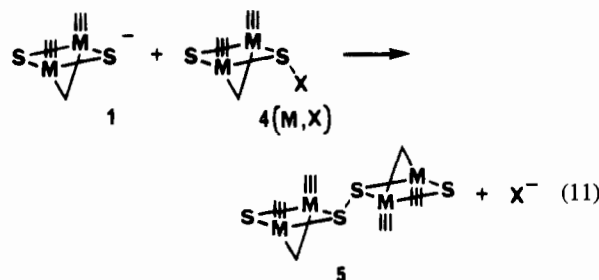
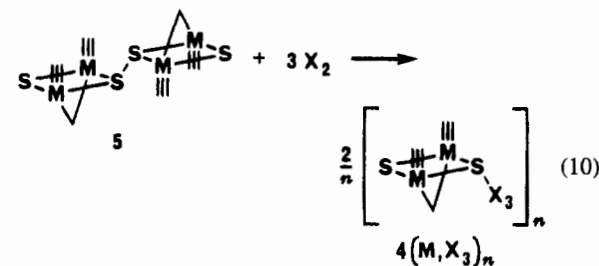
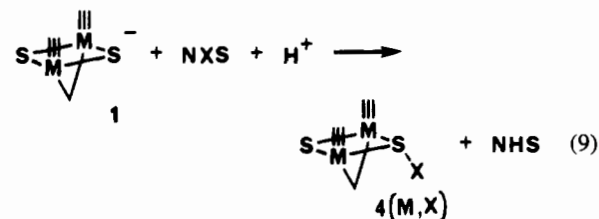
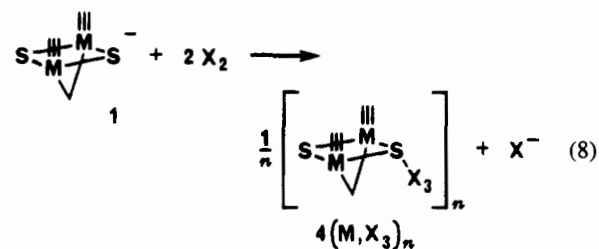
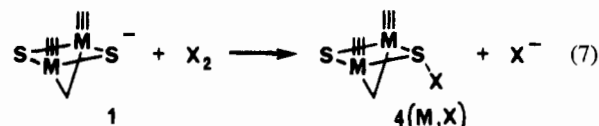
Direct halogenation of sulfur sites within Mo(V) and W(V) dimers was investigated via a number of pathways. Reactions involving the dimer anions  $M_2S^-$ , **1**, proceeded readily although not always cleanly. The anions are typically generated in situ by reactions of tetrameric  $[M(NTO)(S_2P(OEt)_2)_2S]_4$  with acetate, herein provided by  $MeCO_2H/Et_3N$ .<sup>33</sup> For reactions involving

the radicals  $Mo_2S^\bullet$ , **2**, their genesis in situ was via photolysis of the bis-dimer disulfide compound  $Mo_2S-SMo_2$ , **5** (eq 6);



the fluorescent-light induced photohomolysis of  $Mo_2S-SMo_2$  has been previously characterized.<sup>30,32</sup> While photolysis proved necessary for halogenation using  $I_2$ , it became apparent that  $Mo_2S-SMo_2$  reacted directly with  $Br_2$  without photolysis.

Standard halogenation reagents were employed in the current studies, including the elements  $X_2$  (eqs 7, 8, and 10),  $N$ -



halosuccinimides (NXS, eq 9), and *N*-bromophthalimide (analogous to eq 9). For synthetic preparations, the most useful method for each product is given in the Experimental Section, along with several alternate methods which did not fare as well. Other combinations were also examined but generally provided poor results for synthetic applications; for example, direct chlorination of  $W_2S^-$  using  $Cl_2$  gave  $W_2SCl$  but in poor yield.

In many of the reactions, the disulfides  $M_2S-SM_2$  were common byproducts; this was somewhat expected based on eq 11 (above), which parallels the substitution reactions of organic sulfonyl halides ( $RSX$ ) with thiolates ( $RS^-$ ) to give disulfides ( $RSSR$ ).<sup>1,3,5-7</sup>

Products which were isolated included  $W_2SCl$ ,  $W_2SBr$ ,  $W_2SI$ ,  $[W_2SI_3]_n$ ,  $[Mo_2SBr_3]_n$ , and  $[Mo_2SI_3]_n$ . In addition, spectroscopic evidence suggested the successful formation of  $[W_2SBr_3]_n$  and  $Mo_2SCl$ , but these could not be isolated as cleanly characterizable, stable solids. Although  $W_2SX$  products were isolable, no molybdenum monohalide  $Mo_2SX$  could be isolated despite various methods and numerous efforts. Most such efforts were directed at  $Mo_2SI$ , but its isolation was thwarted by its equilibrium with  $[Mo_2SI_3]_n$  and the very poor solubility of the latter. Attempts to avoid  $[Mo_2SI_3]_n$  by using limiting iodine equivalents also failed to obtain isolable  $Mo_2SI$  due to complications from other by-products, including  $Mo_2S-SMo_2$  (cf., eq 11).

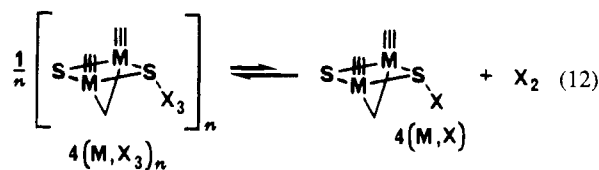
All isolated products were characterized by NMR spectroscopy, IR spectroscopy, and elemental analysis or X-ray crystallography. The  $^1H$  and  $^{31}P$  NMR spectra displayed all appropriate resonances and peaks.<sup>29,31,39,40</sup>  $^{31}P$  NMR spectra also showed  $^{31}P-^{183}W$  couplings for the tungsten derivatives, assignable to  $^2J_{PW}$  (21–22 Hz) and  $^3J_{PW}$  (6–9 Hz). Although compounds of type **3** had frequently shown sulfur inversion isomers in solution, only  $W_2SI$  displayed evidence for such. (The invertomers are portrayed in the structure diagrams for **3** and are labelled distal or proximal based on the orientation of the sulfur substituent relative to the arylimido groups.) Due to overlap in the spectra for  $W_2SI$ , the invertomer ratio (distal/proximal) could at best be estimated as  $\sim 10$ . IR spectra of the various products showed ligand absorptions typical for derivatives containing the  $[M_2(NT_0)_2(S_2P(OEt)_2)_2S_2(O_2CMe)]$  core.<sup>29,31,39,40</sup> In addition,  $\nu(SCl)$  was clearly observed for  $W_2-SCl$  at  $473\text{ cm}^{-1}$  which corresponded with reported  $S-Cl$  stretching frequencies.<sup>10,16,41-46</sup> Definitive assignment of  $\nu(SBr)$  was precluded by the presence of other bands in the  $450-400\text{ cm}^{-1}$  region and the inability to collect data below  $400\text{ cm}^{-1}$  using the instrument on hand; reported values for  $\nu(SBr)$  extend from  $455-385\text{ cm}^{-1}$ .<sup>42-48</sup>  $\nu(SI)$  bands are typically below  $400\text{ cm}^{-1}$ <sup>41-47</sup> and were therefore out of the range of data collection.

The various products exhibit two very different structural types. X-ray crystallography was used to definitively establish the structures of one product of each type, and these results are detailed below. The  $M_2SX$  products,  $4(M,X)$ , are discrete complexes possessing a simple halosulfide bridge,  $\mu-SX$ ; these possess a structure which is similar to those of previous derivatives **3**. The  $[M_2SX_3]_n$  compounds,  $4(M,X_3)_n$ , are one-dimensional polymers containing  $SX_3S$  inter-dimer links to give ...  $M_2S-X-X-X-SM_2S-X-X-X-S$  ... chains.

**Dissociation Equilibrium.** Despite the polymeric nature of solid  $[Mo_2SI_3]_n$ , dissociative processes appeared operative in  $CHCl_3$  solution. This was readily demonstrated by UV-vis spectroscopy. (Solution molecular weight determinations might

have assisted this analysis but these were precluded by very poor solubilities.) For UV-vis spectra of solutions in the concentration range of  $1.00 \times 10^{-4}$  to  $1.00 \times 10^{-5}$  F, plots of absorbance vs concentration were obtained from 430 to 500 nm at 10-nm intervals and showed obvious nonlinearity. (For purpose of UV-vis discussions, concentrations are in terms of  $Mo_2$  units regardless of chain length; likewise,  $\epsilon$  values are per  $Mo_2$  unit regardless of chain length.) The spectrum of the most dilute solution bore semblance to spectra of a variety of  $Mo_2-SZ$  compounds, **3**: published UV-vis spectral parameters of nine such derivatives were similar regardless of the nature of Z ( $Z = R, SR, NH_2$ ).<sup>32</sup> This comparison suggested that at low concentration of  $[Mo_2SI_3]_n$ , depolymerization occurred and produced single, discrete  $Mo_2SI_x$  units of a structure similar to those of **3**. At a high concentration of  $1.00 \times 10^{-3}$  F, however, the UV-vis spectrum of  $[Mo_2SI_3]_n$  clearly differed from those of discrete  $Mo_2SZ$  compounds, showing increased absorption in general, and an additional band appearing near 460 nm.

While indicative of a depolymerization process, these results per se did not identify the equilibrium as that of eq 12 or 13, which differ in the identity of the ultimate, singular  $Mo_2SI_x$



product. It was possible, however, to distinguish between the two possibilities by an analysis of absorbance ratios at 410 and 510 nm ( $A_{410}/A_{510}$ ). These wavelengths approximate the peak positions in the various  $Mo_2SZ$  compounds;<sup>32</sup> furthermore,  $I_2$  has little absorbance at 410 nm ( $\epsilon = 42\text{ cm}^{-1}\text{ M}^{-1}$ ) but appreciable absorbance at 510 nm ( $\epsilon = 938\text{ cm}^{-1}\text{ M}^{-1}$ ). These considerations allowed the distinction to be made based on the derivations given in the Experimental Section. Using data for the previously published compounds  $Mo_2SZ$ , **3**,<sup>32</sup> the calculated absorbance ratios  $A_{410}/A_{510}$  for a hypothetical solution of equimolar, noninteracting,  $Mo_2SZ + I_2$  averaged 2.8; this scenario represented the right side of eq 12. The  $A_{410}/A_{510}$  average was 4.7 as calculated for a  $Mo_2SZ$ -type compound alone, representing the right side of eq 13. For actual solutions of  $[Mo_2SI_3]_n$ ,  $A_{410}/A_{510}$  was 3.7 for concentrations of  $1.00 \times 10^{-3}$  F; this ratio decreased smoothly to 3.2 at  $1.00 \times 10^{-5}$  F. This showed that, upon dilution,  $A_{410}/A_{510}$  tended toward the value for eq 12 and not eq 13, thereby indicating that  $Mo_2SI + I_2$  were the ultimate species upon dilution.

**Charge Transfer Equilibrium.** While covalent halosulfide ligands represented one outcome from the halogenation reactions, it became apparent that the less reactive bridge sulfide sites were capable of charge transfer donation to a halogen acceptor. This was more closely investigated using the ethanethiolate-bridged compound  $Mo_2SEt$ , **3** ( $Z = Et$ ).

The  $^{31}P$  NMR spectroscopic results of the interaction of  $Mo_2SEt$  and various equivalents of  $I_2$  were striking; the spectra are shown in Figure 4. Very small quantities of  $I_2$  produced drastic effects. For  $Mo_2SEt$  by itself, the distal invertomer appeared at 115.2 ppm and the proximal invertomer at 115.0 ppm. With a scant 0.1 equiv of  $I_2$ , the distal peak position jumped upfield

(39) Noble, M. E. *Inorg. Chem.* **1990**, *29*, 1337.

(40) Haub, E. K.; Richardson, J. F.; Noble, M. E. *Inorg. Chem.* **1992**, *31*, 4926.

(41) Bielefeldt, D.; Willner, H. *Spectrochim. Acta* **1980**, *36A*, 989.

(42) Minkwitz, R.; Lekies, R.; Radünz, A.; Oberhammer, H. *Z. Anorg. Allg. Chem.* **1985**, *531*, 31 and references therein.

(43) Minkwitz, R.; Lekies, R. *Z. Anorg. Allg. Chem.* **1985**, *527*, 161.

(44) Minkwitz, R.; Nass, U.; Preut, H. *Z. Anorg. Allg. Chem.* **1986**, *538*, 143.

(45) Minkwitz, R.; Nowicki, J. *Inorg. Chem.* **1990**, *29*, 2361.

(46) Minkwitz, R.; Lekies, R.; Lennhoff, D.; Sawatzki, J.; Kadel, J.; Oberhammer, H. *Inorg. Chem.* **1990**, *29*, 2587.

(47) Minkwitz, R.; Kornath, A.; Preut, H. *Z. Anorg. Allg. Chem.* **1993**, *619*, 877.

(48) Della Vedova, C. O.; Mack, H.-G. *Inorg. Chem.* **1993**, *32*, 948.

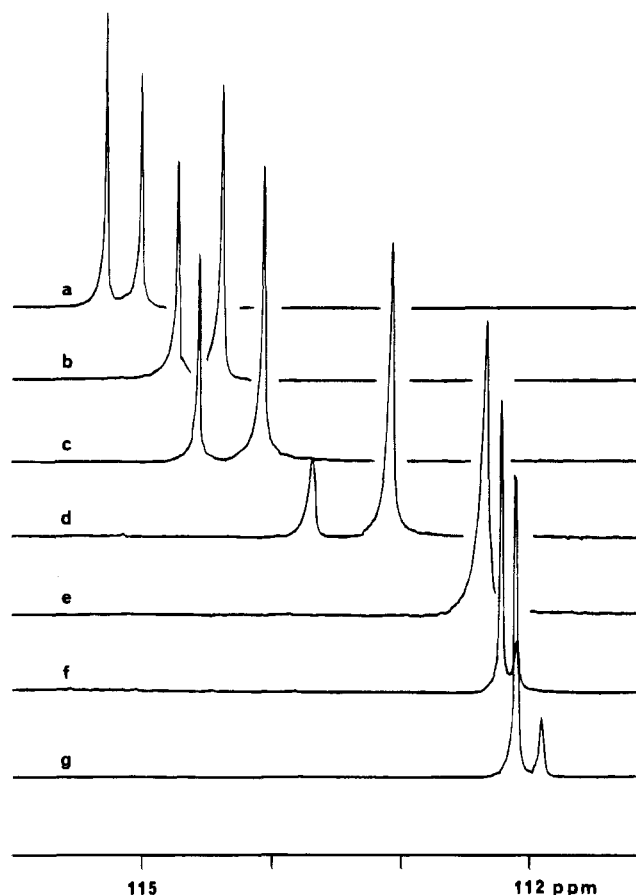


**Figure 4.**  $^{31}\text{P}$  NMR spectra of  $[\text{Mo}_2(\text{NT0})_2(\text{S}_2\text{P}(\text{OEt})_2)_2\text{S}(\text{O}_2\text{CMe})(\text{SEt})]_3$  ( $Z = \text{Et}$ ), with varying amounts of  $\text{I}_2$ : (a) none; (b) 0.1 equiv; (c) 0.2 equiv; (d) 0.4 equiv; (e) 0.6 equiv; (f) 0.8 equiv; (g) 1.0 equiv.

to 114.3 ppm, while the proximal resonance moved more modestly to 114.7 ppm; the result was a crossover of the two peak positions. At 0.2 and again at 0.4 equiv of  $\text{I}_2$ , both resonances were shifting substantially upfield. By 0.6 equiv, however, the shifting of the distal invertomer had slowed relative to that of the proximal invertomer, resulting in fortuitous coincidence at 112.3 ppm. Crossover reoccurred with further  $\text{I}_2$ , as the proximal resonance outpaced the distal resonance upfield. Overall, the results indicated a very favorable charge transfer interaction, with a stronger interaction attributable to the distal invertomer. The invertomer ratios (distal/proximal) also changed during this process, increasing with increasing  $\text{I}_2$  content: with no added  $\text{I}_2$ , the invertomer ratio was 1.3; this increased to 4.8 with 1.0 equiv of  $\text{I}_2$ . The ratio 4.8/1.3 required that the charge transfer equilibrium was  $\sim 3.7$  times greater for the distal than for the proximal isomer.  $^1\text{H}$  NMR spectra also showed shifting of resonances and corroborated the  $^{31}\text{P}$  NMR results, but the shiftings were not as dramatic.

The higher quantities of  $\text{I}_2$  yielded small changes in peak position; with excess  $\text{I}_2$ , some shifting continued, and additional equilibria (e.g., other donor sites or polyiodo interactions<sup>66</sup>) were likely.

Other derivatives also showed charge transfer behavior. The bis-dimer disulfide  $\text{Mo}_2\text{S}-\text{SMo}_2$ , **5**, shifted from 115.8 (distal) and 115.3 ppm (proximal) to 113.7 and 113.5 ppm in the presence of 1.1 equiv of  $\text{I}_2$ . The invertomer ratio increased from 0.13 to 0.4. (This study was conducted under red light conditions<sup>29</sup> to avoid photohomolysis, eq 6, of  $\text{Mo}_2\text{S}-\text{SMo}_2$ .) The tungsten ethanethiolate derivative  $\text{W}_2\text{SEt}$  shifted from 127.5 ppm (proximal) and 127.2 ppm (distal) to 127.0 and 126.2 ppm at 0.25 equiv  $\text{I}_2$ ; the invertomer ratio changed from 0.88 to 1.0. The availability of both  $\text{Mo}_2\text{SEt}$  and  $\text{W}_2\text{SEt}$  allowed a comparative study to determine the relative abilities of the two metal

**Table 4.** Selected Comparative Distances (Å) and Angles (deg)

	prior <b>3</b> <sup>a</sup>	<b>4</b> (W,Br)	<b>4</b> (Mo,I <sub>3</sub> ) <sub>n</sub>
Distances			
M-M	2.8283(6)–2.8336(4) 2.8318	2.8315(6)	2.878(1)
S(1)···S(2)	3.855(2)–3.864(2) 3.859	3.840(5)	3.906(4)
M-S(1)	2.431(1)–2.451(1) 2.442	2.417(3)	2.442(2)
M-S(2)	2.338(1)–2.351(1) 2.346	2.351(3)	2.413(2)
M(1)-S(3) and M(2)-S(5)	2.504(1)–2.520(1) 2.513	2.504(3)	2.501(3)
M(1)-S(4) and M(2)-S(6)	2.550(1)–2.567(2) 2.555	2.536(3)	2.517(3)
M-N	1.721(4)–1.737(4) 1.729	1.743(5)	1.733(6)
M-O	2.171(4)–2.202(2) 2.188	1.753(5)	1.748(6)
		2.187(4)	2.159(5)
		2.177(4)	2.160(5)
Angles			
S(1)-M-S(2)	107.00(5)–107.67(5) 107.42	107.32(9)	107.09(8)
M(1)-S(1)-M(2)	70.731(4)–71.02(3) 70.90	107.02(9)	107.20(8)
M(1)-S(2)-M(2)	74.02(3)–74.38(3) 74.26	71.54(7)	72.30(6)
Sum of angles at tricoordinate S	295.8(2)–296.3(1) 296.0	74.08(8)	73.23(6)
M-N-C	169.2(2)–178.8(4) 174.0	299.0(1)	303.5(1)
		178.4(7)	303.1(1)
		176.6(7)	174.0(6)
			176.5(5)

<sup>a</sup> The specific compounds are listed in the Results. The range is given; below that is the average.

derivatives to charge transfer to iodine. A separate solution of  $\text{Mo}_2\text{SEt} + 0.25 \text{I}_2$  was prepared in  $\text{CDCl}_3$  and the  $^{31}\text{P}$  NMR spectrum was obtained; the quantities matched those of the above  $\text{W}_2\text{SEt} + 0.25 \text{I}_2$  sample. The solutions were then mixed quantitatively, and  $^{31}\text{P}$  NMR data were again obtained. The spectra showed that, after mixing,  $\text{W}_2\text{SEt}$  shifted slightly upfield, while  $\text{Mo}_2\text{SEt}$  shifted slightly downfield. Thus,  $\text{W}_2\text{SEt}$  experienced an increased charge transfer interaction at the expense of  $\text{Mo}_2\text{SEt}$ ; in a competitive situation,  $\text{W}_2\text{SEt}$  was the better charge transfer donor.

**Photochemical Aspects.** The preferred synthesis of  $[\text{Mo}_2\text{SI}_3]_n$  incorporates the photohomolysis, eq 6, of the bis-dimer disulfide  $\text{Mo}_2\text{S}-\text{SMo}_2$ , **5**, to produce radicals  $\text{Mo}_2\text{S}^{\cdot}$ , **2**,<sup>30,32</sup> these then react (at least initially) with  $\text{I}_2$ . Thus, synthesis of  $[\text{Mo}_2\text{SI}_3]_n$  via eq 10 is fluorescent light induced.

$[\text{Mo}_2\text{SI}_3]_n$  itself also proved to be moderately photosensitive. Photolysis of  $[\text{Mo}_2\text{SI}_3]_n$  gave an equilibrium mixture of 67%  $[\text{Mo}_2\text{SI}_3]_n$  and 33%  $\text{Mo}_2\text{S}-\text{SMo}_2$ , with both species charge-transfer shifted due to the  $\text{I}_2$  content. The equilibration was complete after 2 h photolysis, but was not complete after 1 h. Proof of the photoequilibrium was handily obtained by illumination of a corresponding solution of  $\text{Mo}_2\text{S}-\text{SMo}_2 + 3\text{I}_2$ , which gave the same mixture after 2 h. Thus, eq 10 is a fully reversible photoequilibrium for  $X = \text{I}$ ; its utility in the synthesis of  $[\text{Mo}_2\text{SI}_3]_n$  derives from the very poor solubility of this product and its precipitation from solution under the synthetic conditions employed.

**Crystal Structures.** The structures of  $\text{W}_2\text{SBr}$  and of  $[\text{Mo}_2\text{SI}_3]_n$  are shown in Figures 1–3. Metrical results are given in Tables 2 and 3.

The overall structure for  $\text{W}_2\text{SBr}$  is very similar to those previously reported for several molybdenum derivatives  $\text{Mo}_2\text{SZ}$ , **3**. Relevant comparisons are given in Table 4, which includes ranges and averages for prior derivatives  $\text{Mo}_2\text{SSEt}$  **3** ( $Z = \text{SEt}$ ),<sup>49</sup>  $\text{Mo}_2\text{SNH}_2$  **3** ( $Z = \text{NH}_2$ ),<sup>40</sup> and,  $\text{Mo}_2\text{SN}=\text{CHCMe}_3$

3 ( $Z = N=CHCMe_3$ ).<sup>40</sup> In all cases, the imido linkages are linear and the acetates bridge symmetrically. The  $M_2S_2$  cores show distinctly longer M–S bonds to tricoordinate bridge S(1) than to dicoordinate bridge S(2). Bonds to dithiophosphates are inversely influenced by these different sulfur bridge bonds: M–S(dithiophosphate) bonds (M(1)–S(3), M(2)–S(5)) which are trans to the longer bridge bonds are themselves shorter, compared to M–S(dithiophosphate) bonds (M(1)–S(4), M(2)–S(6)) which are trans to the shorter bridge bonds.  $M_2S_2$  cores are planar; the current  $W_2SBr$  shows a dihedral angle of  $177(1)^\circ$  between  $WS_2$  planes.

In addition to the overall features, specific structural details for the dimer portion of  $W_2SBr$  are also very similar to those for the prior molybdenum compounds and differences are modest. Even the W(1)–W(2) bond length is within the range of Mo–Mo bond lengths. The W–S(1) bond lengths are short compared to average Mo–S(1) bond lengths in the previous molybdenum compounds, although the W–S(1) values are near the short end of that range; the modest W–S(1) contraction is supported by a diminished S(1)··S(2) diagonal distance and a slightly wider M(1)–S(1)–M(2) bond angle. Comparing M–S(dithiophosphate) bond lengths, those in  $W_2SBr$  are shorter or at the short end of the range compared to those in  $Mo_2SZ$ . W–N bond lengths are longer than the average for those in  $Mo_2SZ$ , but they are statistically near the long end of the range. The sum of the angles at S(1) is slightly larger for  $W_2SBr$ , which is a steric effect<sup>40</sup> due to the bulky halogen.

An essential feature of  $W_2SBr$  is the bromosulfide bridge unit. The S–Br bond length is 2.209 (2) Å, which is near the sum of the covalent radii (2.18 Å<sup>50</sup>). Comparative structural data for other S–Br compounds is extremely limited, even when including organic and main group derivatives. For two- or three-coordinate sulfur compounds, S–Br structural data have been reported wherein S is also bonded to C, Si, N, O, or another S. For the few which appear to contain discrete S–Br bonds, those bond lengths are in the range of 2.162(6)–2.255(5) Å.<sup>42,44,48,51–53</sup> (Some of these were gas phase measurements.) The range broadens considerably to 2.136(5)–2.449(3) Å for those compounds which also contain charge transfer, ionic, or other contributory influences on the S–Br bond length.<sup>17,54–61</sup> For  $W_2SBr$ , there are no significant intermolecular interactions; the Br··Br distance is 3.77 Å, which approximates twice the van der Waals radius (1.85<sup>62</sup> or 1.95 Å<sup>50</sup>).

The structure of  $[Mo_2SI_3]_n$  is substantially different from that of  $W_2SBr$  and from those of the prior molybdenum derivatives, 3. This is true of the  $Mo_2$  dimer portion itself and of the polymeric nature of the S–I–I–I–S link; these two results are presented separately.

Some of the differences in the dimer portion are a consequence of converting from a  $M_2(\mu-S)(\mu-SZ)$  structure as in 3 (and also as in  $W_2SBr$ ) to a  $M_2(\mu-SZ)_2$  structure; the latter ideally possesses an additional, vertical, mirror plane containing  $M_2N_2O_2$  and other atoms. The individual dimer cores in  $[Mo_2SI_3]_n$  approach such a symmetric ( $C_{2v}$ ) unit, but curiously they retain a portion of the inequivalence of the  $M_2(\mu-S)(\mu-SZ)$  structure. This can be seen by the results in Table 4. The Mo–S(1) bond lengths of  $[Mo_2SI_3]_n$  are very similar to values from previous structures of type 3. Mo–S(2) bond lengths, however, are much longer in  $[Mo_2SI_3]_n$ ; these values approach the Mo–S(1) bond lengths but do not achieve equivalence. The residual inequivalence is manifested also in other parameters such as the Mo–S(dithiophosphate) bonds, the bond lengths within the S–I–I–I–S linkage, and, the Mo(1)–S(1)–Mo(2) and Mo(1)–S(2)–Mo(2) angles.

There are several structural features of  $[Mo_2SI_3]_n$  which differ from the prior derivatives and which are not related to symmetry planes. For example, the Mo–Mo bond is distinctly longer, and, Mo–O bonds are short but statistically near the prior range. The longer Mo–Mo bond and the lengthening of Mo–S(2) bonds gives a larger  $Mo_2S_2$  core which is also reflected in the S(1)··S(2) diagonal distance. The  $Mo_2S_2$  core remains reasonably planar, with  $MoS_2$  planes at  $174^\circ$ . As observed for  $W_2SBr$ , the sums of the angles at tricoordinate sulfur bridges (now S(1) and S(2)) are slightly larger than the values of prior derivatives 3, consistent with a steric effect of the bulky halogen.

The S–I–I–I–S ligands (S(1)–I(1)–I(2)–I(3)–S(2')) link the dimers into a one-dimensional polymer. This unit itself is an unusual structural feature. A number of sulfur-iodine chain compounds have been crystallographically characterized; many of these contain  $SI_x$  ( $x > 1$ ) or  $SI_3S$  units involving S–I and I–I bonds of varying lengths and strengths, ranging from charge transfer distances to nearly single bonds.<sup>63–74</sup> For the iodo chains in these, however,  $x$  and  $y$  are usually even-numbered; this would correspond to a formalism of  $S(I_2)_{x/2}$  or  $S(I_2)_{y/2}S$ , although some S–I–S compounds are known for monovalent iodine(I).<sup>71–74</sup> Despite the dearth of odd- $y$   $SI_3S$  structures, the  $SI_3S^{3-}$  link can be considered isoelectronic and isostructural to the  $I_5^-$  ion, for which several crystal structures have been reported.<sup>75–78</sup>

- (50) Pauling, L. *The Nature of the Chemical Bond*; Cornell University Press: Ithaca, New York, 1960.
- (51) Hirota, E. *Bull. Chem. Soc. Jpn.* **1958**, *31*, 130.
- (52) Brunvoll, J.; Hargittai, I.; Rozsondai, B. *J. Mol. Struct.* **1982**, *84*, 153.
- (53) Passmore, J.; Sutherland, G.; Whidden, T. K.; White, P. S.; Wong, C.-M. *Can. J. Chem.* **1985**, *63*, 1209.
- (54) Allegra, G.; Wilson, G. E., Jr.; Benedetti, E.; Pedone, C.; Albert, R. *J. Am. Chem. Soc.* **1970**, *92*, 4002.
- (55) Kniep, R.; Korte, L.; Mootz, D. *Z. Naturforsch., B: Anorg. Chem., Org. Chem.* **1983**, *38*, 1.
- (56) Marsh, R. E.; Slagle, K. M. *Inorg. Chem.* **1985**, *24*, 2114. The S–Br bond length of 2.449 (3) Å is deduced from information herein.
- (57) Wolmershäuser, G.; Krüger, C.; Tsay, Y.-H. *Chem. Ber.* **1982**, *115*, 1126.
- (58) Hauck, H.-G.; Willing, W.; Müller, U.; Dehnicke, K. *Z. Naturforsch., B: Anorg. Chem., Org. Chem.* **1986**, *41*, 825.
- (59) Minkwitz, R.; Lekies, R.; Preut, H. *Z. Naturforsch., B: Anorg. Chem., Org. Chem.* **1987**, *42*, 1227.
- (60) Minkwitz, R.; Prenzel, H.; Werner, A.; Preut, H. *Z. Anorg. Allg. Chem.* **1988**, *562*, 42.
- (61) Applett, A.; Chivers, T.; Fait, J. F.; Vollmerhaus, R. *Can. J. Chem.* **1991**, *69*, 1022.
- (62) Bondi, A. *J. Phys. Chem.* **1964**, *68*, 441.

- (63) Herbstein, F. H.; Ashkenazi, P.; Kaftory, M.; Kapon, M.; Reisner, G. M.; Ginsburg, D. *Acta Crystallogr., Sect. B: Struct. Sci.* **1986**, *42*, 575 and references therein.
- (64) Tipton, A. L.; Lonergan, M. C.; Stern, C. L.; Shriver, D. F. *Inorg. Chim. Acta* **1992**, *201*, 23.
- (65) Blake, A. J.; Gould, R. O.; Radek, C.; Schröder, M. *J. Chem. Soc., Chem. Commun.* **1993**, 1191.
- (66) Herbstein, F. H.; Schwotzer, W. *J. Am. Chem. Soc.* **1984**, *106*, 2367.
- (67) Freeman, F.; Ziller, J. W.; Po, H. N.; Keindl, M. C. *J. Am. Chem. Soc.* **1988**, *110*, 2586.
- (68) Atzei, D.; Deplano, P.; Trogu, E. F.; Bigoli, F.; Pellinghelli, M. A.; Sabatini, A.; Vacca, A. *Can. J. Chem.* **1989**, *67*, 1416.
- (69) Lu, F. L.; Keshavarz-K., M.; Srdanov, G.; Jacobson, R. H.; Wudl, F. *J. Org. Chem.* **1989**, *54*, 2165.
- (70) Bigoli, F.; Deplano, P.; Mercuri, M. L.; Pellinghelli, M. A.; Trogu, E. F. *Phosphorus Sulfur Silicon* **1992**, *72*, 65.
- (71) Lin, G. H.-Y.; Hope, H. *Acta Crystallogr., Sect. B: Struct. Sci.* **1972**, *28*, 643.
- (72) Nosco, D. L.; Heeg, M. J.; Glick, M. D.; Elder, R. C.; Deutsch, E. J. *Am. Chem. Soc.* **1980**, *102*, 7784.
- (73) Passmore, J.; Sutherland, G.; White, P. S. *Inorg. Chem.* **1982**, *21*, 2717.
- (74) Demartin, F.; Deplano, P.; Devillanova, F. A.; Isaia, F.; Lippolis, V.; Verani, G. *Inorg. Chem.* **1993**, *32*, 3694.
- (75) Broekema, J.; Havinga, E. E.; Wiebenga, E. H. *Acta Crystallogr.* **1957**, *10*, 596. Hach, R. J.; Rundle, R. E. *J. Am. Chem. Soc.* **1951**, *73*, 4321.
- (76) Neupert-Laves, K.; Dobler, M. *Helv. Chim. Acta* **1975**, *58*, 432.
- (77) Beno, M. A.; Geiser, U.; Kostka, K. L.; Wang, H. H.; Webb, K. S.; Firestone, M. A.; Carlson, K. D.; Nuñez, L.; Whangbo, M.-H.; Williams, J. M. *Inorg. Chem.* **1987**, *26*, 1912.
- (78) Zhang, W.; Wilson, S. R.; Hendrickson, D. N. *Inorg. Chem.* **1989**, *28*, 4160.



The S—I bond lengths in  $[\text{Mo}_2\text{SI}_3]_n$  of 2.498(2) and 2.544(2) Å are longer than the sum of covalent radii (2.37 Å<sup>50</sup>). S—I bond lengths to terminal iodines are known down to 2.30 Å in sulfur-iodine binary cations.<sup>14</sup> The S—I bond length in  $\text{Ph}_3\text{-CSI}$  is 2.406 (4) Å, although there are intermolecular contacts in that structure.<sup>79</sup> Some thione-iodine complexes contain considerably covalent S—I bonds;<sup>66</sup> S—I bond lengths in those compounds extend to 2.487(3) Å. The I—I bond lengths in  $[\text{Mo}_2\text{SI}_3]_n$  of 3.1584(7) and 3.0363(8) Å are longer than twice the iodine covalent radius (sum 2.66 Å<sup>50</sup>); these are, however, within the ranges for  $\text{I}_5^-$  ions<sup>75-78</sup> and for  $\text{SI}_3\text{S}$  compounds with appreciably covalent S—I bonds.<sup>66</sup> Overall, the bond lengths in the S—I—I—I—S unit show inequivalence, with the longer S—I bond associated with the shorter I—I bond and vice versa. This inverse bond length relationship parallels a pattern established for other compounds containing  $\text{SI}_x$  or  $\text{SI}_3\text{S}$  units,<sup>65,66,68</sup> and the values for  $[\text{Mo}_2\text{SI}_3]_n$  do indeed fit the curve previously reported for S—I vs I—I bond lengths.<sup>66</sup> The bond angles within the S—I—I—I—S linkage also parallel the pattern for  $\text{SI}_x$  and  $\text{SI}_3\text{S}$  compounds and for  $\text{I}_5^-$  ions: the central I—I—I angle is nearly perpendicular (83.89 (2)°), while S—I—I angles are nearly linear (171.65 (5)° and 172.65 (4)°).

The S—I—I—I—S unit is planar with displacements of 0.01 Å or less. This plane is perpendicular to the  $\text{Mo}_2\text{S}_2$  plane.

## Discussion

The reactions and interactions of halogens with metallosulfur sites as described herein proved to be rather diverse, with products ranging from discrete metallosulfenyl halides,  $\text{M}_2\text{SX}$ , to charge transfer systems,  $\text{X}_2 \cdot \text{SM}_2\text{SZ}$ , with these two extremes bridged by the  $\text{SXXXS}$  chains of the  $[\text{M}_2\text{SX}_3]_n$  derivatives.

The metallosulfenyl halides,  $\text{M}_2\text{SX}$ , show reasonable parallel to organic sulfenyl halides,  $\text{RSX}$ . The order of apparent stabilities is somewhat reversed: for  $\text{RSCI}$ ,  $\text{RSBr}$ , and  $\text{RSI}$ ,<sup>1,5-7,12</sup> the chlorides are best established and most readily isolable; isolable  $\text{RSI}$  derivatives are rare, and disproportionation (to  $\text{RSSR} + \text{I}_2$ ) is much more common. Of the present  $\text{M}_2\text{SX}$ , only tungsten derivatives could be isolated, and  $\text{W}_2\text{SCI}$  was the least stable. The ability to isolate  $\text{W}_2\text{SI}$  may be a steric result: many of the few isolable  $\text{RSI}$  compounds contain bulky R groups, the significance of which has been addressed mechanistically.<sup>7</sup>

The charge transfer interactions studied herein involve the "back-bridge" sulfur site of  $\text{M}_2\text{SZ}$  compounds to give  $\text{I—I} \cdot \text{SMO}_2\text{-SZ}$ . The back-bridge sulfide is a site of modest reactivity in these and related compounds.<sup>33,80</sup> The current studies revealed a clear preference for the distal invertomer to act as charge transfer donor relative to the proximal invertomer. This result is explained by structural differences between distal and proximal isomers in  $\text{Mo}_2\text{SZ}$  derivatives: the  $\text{Mo}_2\text{S}_2$  core is planar in distal isomers, but in the proximal isomer, the tricoordinate sulfur bridge ( $\mu\text{-SZ}$ ) drops well out of the plane (by more than 0.2 Å).<sup>40</sup> The planarity in the distal isomer implies  $\pi$  contributions from both the sulfide back-bridge and the tricoordinate sulfur bridge sites. In the proximal isomer, the  $\pi$  contribution from tricoordinate sulfur is diminished; this places greater demand on the back-bridge sulfide site and leaves less electron density for charge transfer donation.

The interactions of  $\text{X}_2$  with the bis-dimer disulfide  $\text{Mo}_2\text{S—SMO}_2$  provided an interesting comparison. For  $\text{X} = \text{I}$ , charge transfer occurred to give  $\text{I—I} \cdot \text{SMO}_2\text{S—SMO}_2$  interactions, possibly in equilibrium with some  $\text{I—I} \cdot \text{SMO}_2\text{S—SMO}_2\text{S} \cdot \text{I—}$

$\text{I}$ ; this was a thermal process. In light,  $\text{I}_2 + \text{Mo}_2\text{S—SMO}_2$  gave iodosulfide product via radicals  $\text{Mo}_2\text{S}^*$ . For the more aggressive  $\text{Br}_2$ , however, direct halogenation occurred in the dark to give bromosulfide product. Mechanistically, this process may involve attack of  $\text{Br}_2$  on the back-bridge sulfide site, facilitated by an initial charge transfer interaction,  $\text{Br—Br} \cdot \text{SMO}_2\text{S—SMO}_2$ . Direct attack of  $\text{Br}_2$  on the S—S linkage of  $\text{Mo}_2\text{S—SMO}_2$  is unlikely, since this disulfide bond is buried and is unavailable to direct attack by disulfide reagents.<sup>30</sup>

The trihalides  $[\text{M}_2\text{SX}_3]_n$  represent a link between the covalent  $\text{M}_2\text{SX}$  structure and the simple charge transfer system  $\text{X—X} \cdot \text{SM}_2\text{SZ}$ . The one-dimensional polymer chain can be considered to contain a contribution from a structure such as  $\cdot \text{SM}_2\text{S—X} \cdot \text{X—X} \cdot \text{SM}_2\text{S—X} \cdot \text{X—X}$ . This is evident in the inequivalent and alternating bond lengths revealed in the crystal structure of  $[\text{Mo}_2\text{SI}_3]_n$ , and, it is also supportive of, and supported by, the dissociative equilibrium (eq 12) to give  $\text{Mo}_2\text{-SI} + \text{I}_2$ . The dissociation of eq 12 is actually a limiting case:  $\text{Mo}_2\text{SI} + \text{I}_2$  was shown to be the ultimate equilibrium species at high dilution. This does not eliminate  $\text{Mo}_2\text{SI}_3$  as a component species which also equilibrates to  $\text{Mo}_2\text{SI} + \text{I}_2$ . There are actually two possibilities for such a  $\text{Mo}_2\text{SI}_3$ -type compound: a covalent sulfenyl triiodide,  $\text{Mo}_2(\mu\text{-SI}_3)$ , or a charge transfer interaction of the type  $\text{I—I} \cdot \text{SMO}_2\text{SI}$ . The charge transfer scenario parallels the behavior of the other  $\text{Mo}_2\text{SZ}$  compounds; a sulfenyl triiodide is more speculative, although  $\text{RSI}_3$  compounds have been considered in protein sulfenyl iodide studies.<sup>12</sup>

While some of the chemistry described herein has considerable parallel with organic sulfur and with main group sulfur chemistry, there is little transition metal precedent. A greater generality can perhaps be anticipated, however: for example, reactions of metallosulfur complexes with  $\text{X}_2$  have been frequently reported.<sup>24,72,81-90</sup> These can involve halosulfide intermediates although ultimate products may not contain  $\text{SX}$  bonds. The possible intermediacy of a halosulfide ligand was specifically mentioned in a few cases.<sup>85,86</sup> One  $\text{SI}$  and  $\text{SBr}$  ligand has been specifically proposed in  $[(\text{C}_5\text{Me}_5)_2\text{Cr}_2\text{S}_4\text{X}_2]$  compounds, but these could not be crystallographically characterized;<sup>89</sup> the reported descriptions of the related " $(\text{C}_5\text{Me}_5)_2\text{-Mo}_2\text{S}_4\text{I}_2$ " also suggests the  $\text{SI}$  ligand.<sup>88,90</sup> The present crystal structure of the  $\text{W}_2\text{SBr}$  complex **4**( $\text{W,Br}$ ) definitively establishes this ligand type. The present crystal structure of  $[\text{Mo}_2\text{SI}_3]_n$  **4**( $\text{Mo,I}_3$ ) illustrates another possible product in these reactions. The crystal structure of a complex between  $\text{I}_2$  and another imido-sulfidomolybdenum(V) complex has also been reported;<sup>87</sup> that structure contained a very long  $\text{S} \cdot \text{I}$  bond of 2.720(1) Å and was a simple charge transfer interaction. Interestingly, it also fits the curve previously reported for organic S—I vs I—I relationships,<sup>66</sup> although it lies more to the charge transfer region of the curve than the present, more covalent  $[\text{Mo}_2\text{SI}_3]_n$ . These S—I—I relationships are therefore very general and clearly

(79) Minkwitz, R.; Preut, H.; Sawatzki, J. Z. *Naturforsch., B: Anorg. Chem., Org. Chem.* **1988**, *43*, 399.

(80) Wang, R.; Koffi-Sokpa, E.; Davis, J. L.; Noble, M. E. Work in progress.

(81) Farrar, D. H.; Grundy, K. R.; Payne, N. C.; Roper, W. R.; Walker, A. *J. Am. Chem. Soc.* **1979**, *101*, 6577.

(82) Brunner, H.; Merz, A.; Pfauntsch, J.; Serhadli, O.; Wachter, J.; Ziegler, M. L. *Inorg. Chem.* **1988**, *27*, 2055.

(83) Coucouvanis, D.; Toupadakis, A.; Hadjikyriacou, A. *Inorg. Chem.* **1988**, *27*, 3272.

(84) Amarasekera, J.; Rauchfuss, T. B. *Inorg. Chem.* **1989**, *28*, 3875.

(85) Ramasami, T.; Taylor, R. S.; Sykes, A. G. *Inorg. Chem.* **1977**, *16*, 1931.

(86) Ansari, M. A.; Chandrasekaran, J.; Sarkar, S. *Polyhedron* **1988**, *7*, 471.

(87) Allshouse, J.; Haltiwanger, R. C.; Allured, V.; Rakowski DuBois, M. *Inorg. Chem.* **1994**, *33*, 2505.

(88) Brunner, H.; Meier, W.; Wachter, J.; Weber, P.; Ziegler, M. L.; Enemark, J. H.; Young, C. G. *J. Organomet. Chem.* **1986**, *309*, 313.

(89) Brunner, H.; Pfauntsch, J.; Wachter, J.; Nuber, B.; Ziegler, M. L. *J. Organomet. Chem.* **1989**, *359*, 179.

(90) Brunner, H.; Grassl, R.; Wachter, J.; Nuber, B.; Ziegler, M. L. *J. Organomet. Chem.* **1992**, *427*, 57.

demonstrate that the elements S and I themselves control these structures regardless of organosulfur or metallosulfur framework.

Some metal compounds have been reported wherein halogen weakly binds more than one sulfur: these include a Co–S(R)–I–S(R)–Co complex which contains dicoordinate iodine(I)<sup>72</sup> and several *triangulo* Mo<sub>3</sub> complexes which contain X–(S<sub>2</sub>)<sub>3</sub> interactions.<sup>91–95</sup> These represent examples in addition to [Mo<sub>2</sub>–SI<sub>3</sub>]<sub>n</sub> which involve sulfur–halogen structural modes which lie between simple charge transfer and strongly covalent metallosulfenyl halide systems.

A complication facing studies of metallosulfenyl halides is the possibility for light sensitivity. The present [Mo<sub>2</sub>SI<sub>3</sub>]<sub>n</sub> was only modestly sensitive to fluorescent light, compared to Mo<sub>2</sub>S–

SMo<sub>2</sub> or Mo<sub>2</sub>S–SR derivatives; some of these latter compounds are very sensitive to normal room lighting and their solutions must be handled under red light.<sup>30,32</sup> Organic sulfenyl halides, RSX, are photosensitive, although these typically require UV (some near-UV) irradiation.<sup>96,97</sup>

**Acknowledgment.** This work was supported by research awards from the National Science Foundation, the Kentucky EPSCoR program, and the Department of Education GAANN Program.

**Supporting Information Available:** Tables of full crystallographic parameters, positional parameters, bond lengths, bond angles, displacement parameters, and, least-squares planes (23 pages). This material is contained in many libraries on microfiche, immediately follows this article in the microfilm version of the journal, and can be ordered from the ACS; see any current masthead page for ordering information.

IC950768Y

- 
- (91) Maoyu, S.; Jinling, H.; Jiaxi, L. *Acta Crystallogr., Sect. C: Cryst. Struct. Commun.* **1984**, *40*, 759.  
(92) Klingelhöfer, P.; Müller, U.; Friebel, C.; Pebler, J. *Z. Anorg. Allg. Chem.* **1986**, *543*, 22.  
(93) Fedin, V. P.; Mironov, Y. V.; Virovets, A. V.; Podberezskaya, N. V.; Fedorov, V. Y. *Polyhedron* **1992**, *11*, 2083.  
(94) Borgs, G.; Keck, H.; Kuchen, W.; Mootz, D.; Wiskemann, R.; Wunderlich, H. *Z. Naturforsch., B: Anorg. Chem., Org. Chem.* **1991**, *46*, 1525.  
(95) Meienberger, M. D.; Hegetschweiler, K.; Rügger, H.; Gramlich, V. *Inorg. Chim. Acta* **1993**, *213*, 157.

---

(96) Block, E. *Q. Rep. Sulfur Chem.* **1969**, *4*, 237.

(97) Horspool, W. M. In *The Chemistry of Sulphenic Acids and their Derivatives*; Patai, S., Ed.; Wiley & Sons: Chichester, England, 1990; p 517.